Journal of Alloys and Compounds 489 (2010) 175–178

Contents lists available at ScienceDirect

Journal of Alloys and Compounds

journal homepage: www.elsevier.com/locate/jallcom

Phase transition behavior and electrical properties of $[(K_{0.50}Na_{0.50})_{1-x}Ag_x](Nb_{1-x}Ta_x)O_3$ lead-free ceramics

Yuanyu Wang*, Liu Qibin, Fei Zhao

College of Materials Science and Metallurgy Engineering, Guizhou University, Guiyang 550003, PR China

ARTICLE INFO

Article history:
Received 21 May 2009
Received in revised form 8 September 2009
Accepted 9 September 2009
Available online 16 September 2009

Keywords:
Lead-free piezoelectric ceramics
$(K_{0.5}Na_{0.5})NbO_3$
Phase transition behavior
Piezoelectric properties

ABSTRACT

The effect of $AgTaO_3$ on the electrical properties of $(K_{0.5}Na_{0.5})NbO_3$ lead-free ceramics was systematically investigated, and the phase transition behavior of the ceramics was also studied in terms of high temperature X-ray diffraction. The experimental results show that Ag^+ and Ta^{5+} ions diffuse into the $(K_{0.5}Na_{0.5})NbO_3$ lattices to form a stable solid solution with orthorhombic structure, and also lead to the decrease in the orthorhombic to the tetragonal phase transition temperature and the Curie temperature. The $0.92(K_{0.5}Na_{0.5})NbO_3$–$0.08AgTaO_3$ ceramics exhibit optimum electrical properties (d_{33} = 183 pC/N, k_p = 41%, T_c = 356 °C, T_{o-t} = 158 °C, $\varepsilon_r \sim 683$, and $\tan\delta \sim 3.3\%$) and good thermal-depoling behavior. The piezoelectric properties of $(1-x)(K_{0.5}Na_{0.5})NbO_3$–$xAgTaO_3$ ceramics are much superior to pure $(K_{0.5}Na_{0.5})NbO_3$ ceramics. X-ray diffraction patterns for the $0.92(K_{0.5}Na_{0.5})NbO_3$–$0.08AgTaO_3$ ceramic at different temperatures indicated a pure perovskite phase with an orthorhombic structure at below 160 °C, a tetragonal structure at 160–350 °C, and a cubic structure at above 360 °C. As a result, the $(1-x)(K_{0.5}Na_{0.5})NbO_3$–$xAgTaO_3$ ceramic is one of the promising candidate materials for lead-free piezoelectric ceramics.

1. Introduction

Perovskite $Pb(Zr_xTi_{1-x})O_3$ piezoelectric ceramics were widely used. However, the use of the lead-based piezoelectric ceramics has caused seriously environmental and health problems because of the high toxicity of lead oxide. In recent years, some countries have also required all new electronic products to be lead-free for the environmental protection and human health. Therefore, considerable attention for lead-free piezoelectric materials has been recently given to $(K_{0.50}Na_{0.50})NbO_3$ (KNN)-based ceramics for their excellent piezoelectric properties, high Curie temperature, and environmental friendliness [1–20].

It is well known that pure KNN ceramics are usually difficult to densify by normal sintering for the volatility of alkaline elements at high sintering temperatures, and so the KNN ceramics prepared by normal sintering usually exhibit poor piezoelectric properties (d_{33} = 80 pC/N and k_p = 0.36) [1]. In order to improve the densification and piezoelectric properties of KNN ceramics, the different additions were added into KNN to form new KNN-based ceramic systems, such as KNN–$LiNbO_3$ [4], KNN–$LiSbO_3$ [8,15], KNN–$(Bi_{0.5}Na_{0.5})TiO_3$ [18], and KNN–$LiNbO_3$–$(Ag_{0.5}Li_{0.5})TaO_3$ [12]. However, there were few reports on the phase transition behavior and piezoelectric properties of $AgTaO_3$-modified $(K_{0.5}Na_{0.5})NbO_3$ lead-free piezoelectric ceramics. Generally, the ion radius of Ag is very similar to that of $(K_{0.5}Na_{0.5})^+$. Moreover, it was also reported that Ag or Ta ion can improve the piezoelectric properties [6,10]. Therefore, in the present work, $AgTaO_3$-modified $(K_{0.5}Na_{0.5})NbO_3$ lead-free piezoelectric ceramics were prepared by the ordinary solid-state sintering, their phase transition behavior and piezoelectric properties were mainly studied, and the thermal-depoling behavior of these ceramics was also investigated. The results show that the $AgTaO_3$ improves the piezoelectric properties of $(K_{0.5}Na_{0.5})NbO_3$ ceramics.

2. Experimental

The $(1-x)(K_{0.5}Na_{0.5})NbO_3$–$xAgTaO_3$ [$(1-x)$KNN–xAT] (x = 0, 0.01, 0.02, 0.03, 0.04, 0.05, 0.06, 0.07, 0.08, 0.09, 0.010, 0.012) lead-free ceramics were prepared by the conventional mixed-oxide method. Na_2CO_3 (99.8%), K_2CO_3 (99%), Nb_2O_5 (99.5%), Ag_2O (99%), and Ta_2O_5 (99.99%) are used as the starting raw materials. All materials were ball milled for 36 h with agate ball media and alcohol. After calcination at 850–950 °C for 10 h, the calcined solid solution powders were again milled for 24 h, and pressed into disks of 1.5 cm diameter and 0.6–1.3 mm thickness at 20 MPa using polyvinyl alcohol (PVA) as a binder. These ceramics were sintered at 1100–1200 °C after burning off PVA. Silver paste was sintered on both sides of the samples at 650 °C for 10 min to form electrodes for the electrical measurements. The samples were poled in a 20–150 °C silicon oil bath by applying the direct current electric field of 4 kV/mm for 30 min.

X-ray diffraction (XRD) characterization of the ceramics was performed by Cu Kα radiation (λ = 1.54178 Å) in the θ–2θ scan mode. Phase transition behavior of the ceramics was studied by high temperature X-ray diffraction. The bulk density of the ceramics was measured by the Archimedes method. The temperature dependence

* Corresponding author.
E-mail address: yuanyuwang0216@163.com (Y. Wang).

0925-8388/$ – see front matter © 2009 Elsevier B.V. All rights reserved.
doi:10.1016/j.jallcom.2009.09.047

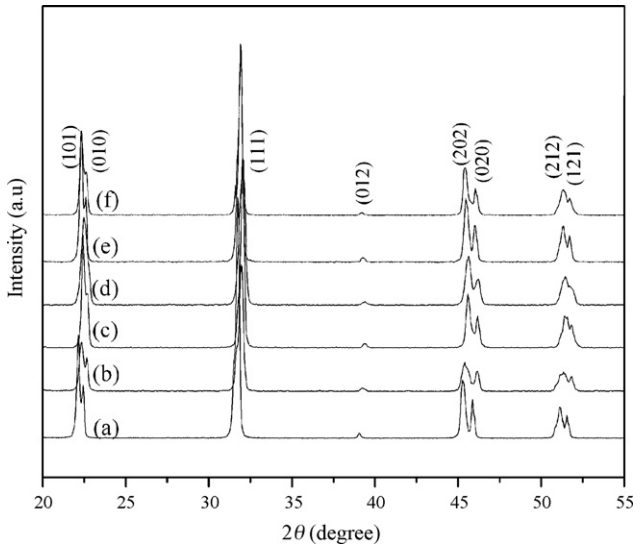

Fig. 1. XRD patterns of the $(1-x)$KNN–xAT ceramics as a function of x. (a) $x=0$; (b) $x=0.04$; (c) $x=0.08$; (d) $x=0.09$; (e) $x=0.10$; (f) $x=0.12$.

of the dielectric constant of the ceramics was examined by a programmable furnace with an *LCR* analyzer. The piezoelectric constant was measured by a piezo-d_{33} meter (ZJ-3A, China). The electromechanical coupling factor k_p of the ceramics was determined by the resonance method using an impedance analyzer.

3. Results and discussion

Fig. 1 shows the XRD patterns of $(1-x)$KNN–xAT ceramics as a function of x. It was found from Fig. 1 that all the ceramics exhibit a perovskite structure with orthorhombic symmetry, and no secondary phases were formed in the range detected. Moreover, the positions of the diffraction peak of the ceramics shift to higher angles with the increase of x. Therefore, the geometrical distortion of the ceramics was induced by a part of AT substitution for KNN. As a result, the introduction of AT did not change the crystal structure of KNN ceramics, and only resulted in the geometrical distortion of the ceramics.

In order to confirm the phase transitional behavior of 0.92KNN–0.08AT ceramics, XRD patterns of 0.92KNN–0.08AT ceramics were measured at different temperatures by high temperature XRD, where the measurement was carried out after holding time for 30 min at each chosen temperature, which made sure that the sample was homogeneously heated. Fig. 2 shows the XRD patterns of the 0.92KNN–0.08AT ceramics at the range of T from 25 to 400 °C. As shown in Fig. 2, the phase structure of the 0.92KNN–0.08AT ceramic changes with measurement temperature, where two different phase transitions were clearly observed, i.e., the orthorhombic structure at below 160 °C, the tetragonal structure at 160–350 °C, and the cubic structure at above 360 °C. Fig. 3 shows enlarged XRD patterns of the 0.92KNN–0.08AT ceramic at different temperatures in the range of 2θ from 21° to 24° and from 44° to 47°. The orthorhombic phase is usually characterized by two peaks splitting at about 22° and 45°; the tetragonal phase is also characterized by peak splitting about 22° and 45°, but the intensity of two peaks differs from that of orthorhombic phase; the cubic structure is characterized by only one peak at about 22°. All results were shown in Fig. 3(a) and (b). Therefore, it was thought that the phase structure of the 0.92KNN–0.08AT ceramic transforms from orthorhombic phase to tetragonal phase, then to cubic phase with the further increase of temperature.

Fig. 4(a) shows the change in the relative density of the $(1-x)$KNN–xAT ceramics as a function of x. It was found that the relative density increases with the increase of x, reaches maximum

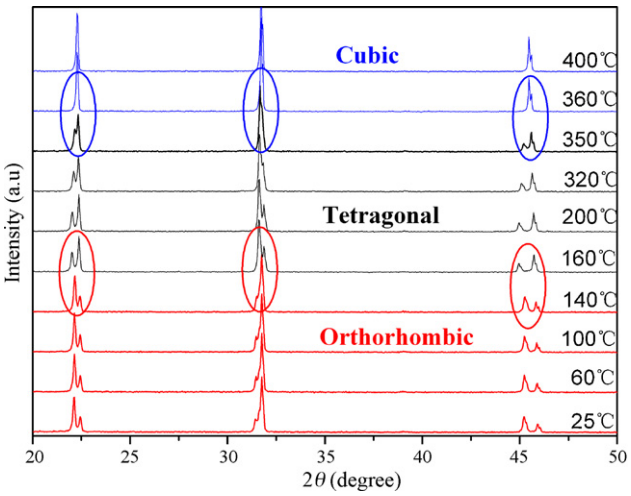

Fig. 2. XRD patterns of 0.92KNN–0.08AT ceramics at different temperatures.

(96.8%) at $x=0.08$. However, the density decreases with the further increase of the AT. In this work, the sintering temperature of $(1-x)$KNN–xAT increases with the increase of AT concentration, too high sintering temperature will result in the volatilization of some element in the KNN ceramics, and therefore the density decreases at high concentration of AT. Optimum AT concentration made KNN ceramic denser, as indicated in Fig. 4(b) and (c). Therefore, the densification of the ceramics was obviously improved by adding optimum AT. Fig. 4(b) and (c) shows SEM patterns of the cross-sectional and surface morphology of the $(1-x)$KNN–xAT ceramics with $x=0.08$. It shows that the ceramics with $x=0.08$ exhibit dense microstructure, where small grains are surrounding the big grains. As a result, the high density should be attributed to the dense microstructure caused by optimum AT concentration, and the high density may also improve the piezoelectric properties of $(1-x)$KNN–xAT ceramics, which will discussed later.

Fig. 5(a) and (b) shows the piezoelectric constant d_{33}, electromechanical coefficient k_p, dielectric constant ε_r, and dielectric loss $\tan\delta$ of the ceramics as a function of x. It is found from Fig. 5(a) that the d_{33} value increases with the increase of x, reaches max-

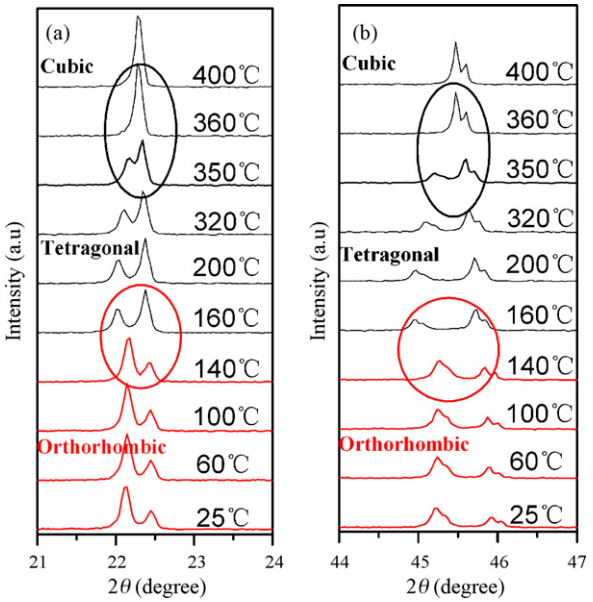

Fig. 3. Enlarged XRD patterns of 0.92KNN–0.08AT ceramics at different temperatures in the range of 2θ (a) from 21° to 24° and (b) from 44° to 47°.

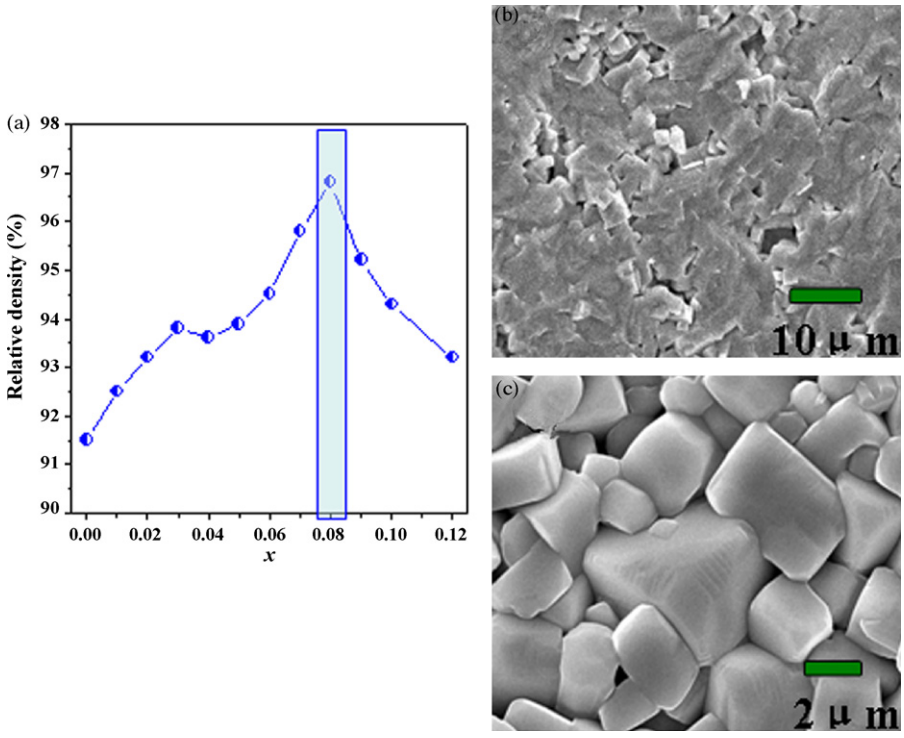

Fig. 4. (a) Relative density of the ceramics as a function of x, (b) cross-sectional and (c) surface morphology of the ceramics with $x = 0.08$.

imum (183 pC/N) at $x = 0.08$, and then decreases with the further increase of x. The piezoelectric properties of the ceramics are much double higher than that ($d_{33} = 80$ pC/N and $k_p = 0.36$) of pure KNN ceramics reported by other authors [1]. Similarly to the change of d_{33}, the k_p value also reaches a maximum value (41%) at $x = 0.08$. In this work, good piezoelectric properties should be attributed to the dense microstructure and the optimum $AgTaO_3$ substitution. Moreover, the ε_r value increases with the increase of x, which also proves that there is no any phase transitions in the ceramics at room temperature. This result is in agreement with the crystal structure of $(1-x)$KNN–xAT ceramics in Fig. 1. The tan δ value of the ceramics decreases with doping AT, then there are almost no changes at $x = 0.01$–0.09, and however steadily increases at $x > 0.09$ for the decrease of the density. The change of the tan δ value is related to the density of $(1-x)$KNN–xAT ceramics. These results indicate the ceramics with $x = 0.08$ possess optimum piezoelectric and dielectric properties at room temperature ($d_{33} = 183$ pC/N, $k_p = 41\%$, $\varepsilon_r \sim 683$, and tan $\delta \sim 3.3\%$).

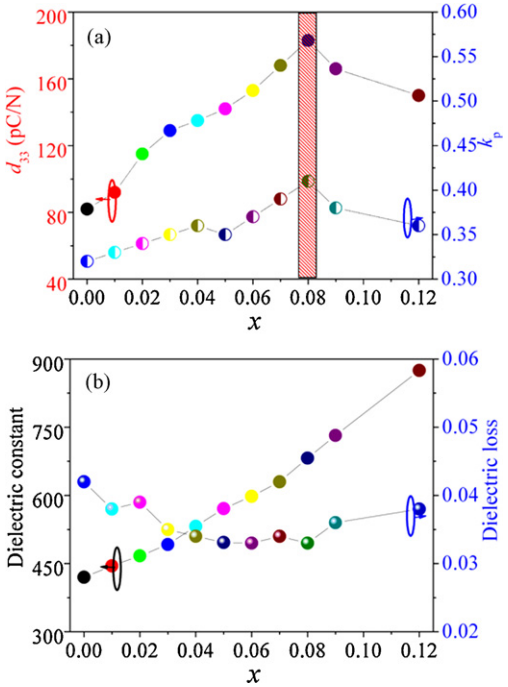

Fig. 5. (a) Piezoelectric properties and (b) dielectric properties of the $(1-x)$KNN–xAT ceramics as a function of x.

The temperature dependence of the ε_r for the ceramics measured at 10 kHz is shown in Fig. 6(a). As shown in Fig. 6(a), two peaks were clearly observed from these curves, i.e., the tetragonal and cubic phase transition temperature (T_c) and the orthorhombic and tetragonal phase transition temperature (T_{o-t}). The result is corresponding to the phase transition measured by high temperature XRD. Moreover, it was observed that $AgTaO_3$ decreases the T_c and T_{o-t} values of the ceramics. Fig. 6(b) shows the T_c and T_{o-t} of the ceramics as a function of x. As shown in Fig. 6(b), the observed T_c decreases from 423 to 313 °C as x increases from 0.00 to 0.12, and the T_{o-t} also decreases from 210 to 128 °C as x increases from 0.00 to 0.12. As a result, AT decreases the Curie temperature and the polymorphic orthorhombic–tetragonal phase transition temperature of these ceramics.

The thermal-depoling behavior of the piezoelectric properties of the ceramics is very important for the practical application in devices. The thermal-depoling behavior of the d_{33} and ε_r values of the ceramics with $x = 0.08$ was shown in Fig. 7(a). Among these, the d_{33} values were measured at room temperature after annealing for 2 h at each chosen annealing temperature (T_a). It can be observed from this figure that the d_{33} value shows a slight variation when the T_a is lower than T_c. However, when the T_a is close to T_c, the d_{33} rapidly decreases, and even disappears when the T_a was above T_c. Fig. 7(b) shows the thermal-depoling behavior of the k_p and ε_r of the ceramics with $x = 0.08$. Similarly to the changes of the d_{33}, the k_p value shows a slight variation when the T_a is lower than T_c. However, when the T_a is close to T_c, the k_p rapidly decreases, and

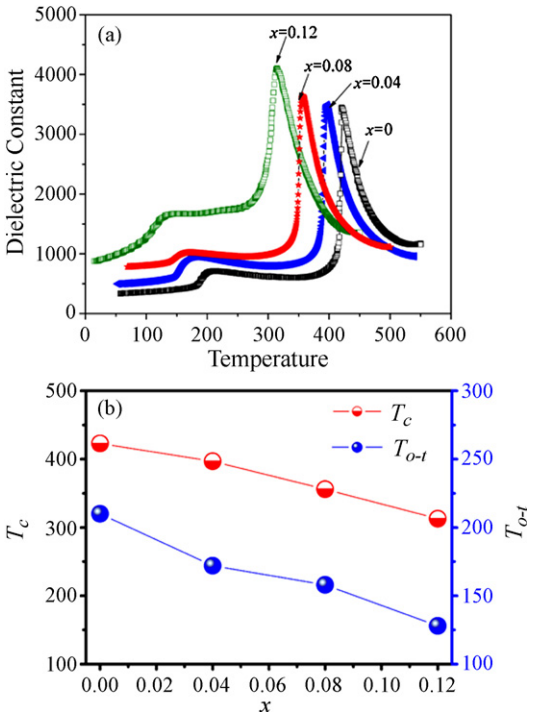

Fig. 6. (a) Temperature dependence of the dielectric constant for $(1-x)$KNN–xAT ceramics at 10 kHz: (b) T_c and T_{o-t} of the ceramics as a function of x.

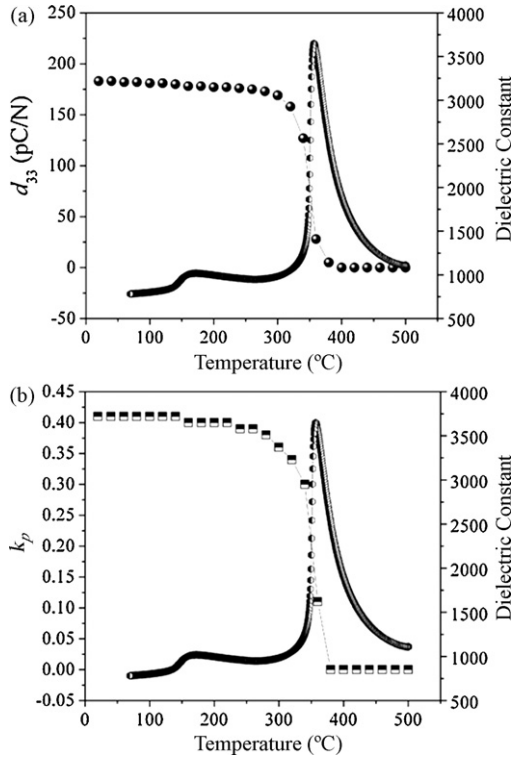

Fig. 7. (a) Thermal-depoling behavior and of the d_{33} and ε_r of the ceramics with $x = 0.08$, (b) thermal-depoling behavior of the k_p and ε_r of the ceramics with $x = 0.08$.

even disappears when the T_a was above T_c. These results show that the ceramics possess good thermal-depoling characteristics.

It is generally thought that the enhancement of the piezoelectric properties for the KNN ceramics is mainly attributed to the coexistence of orthorhombic and tetragonal phases because the ceramics with the coexistence of two phases possess more possible polarization states [5,6,8]. However, for the $(1-x)$KNN–xAT ceramics, phase transitions do not happen at room temperature. As a result, the improvement of the piezoelectric properties of the KNN–AT ceramics should not be attributed to the coexistence of two phases. Therefore, enhanced piezoelectric properties at room temperature ($d_{33} = 183$ pC/N and $k_p = 41\%$) should be attributed to optimum AT concentration, where denser microstructure (Fig. 4) is also partly responsible for the improvement of the piezoelectric properties. Other possible reason may be partly attributed to the appropriate distortion which may introduce by doping AT (Fig. 1), which also results in the enhancement of the piezoelectric properties.

4. Conclusions

$(1-x)(K_{0.50}Na_{0.50})NbO_3$–$x$AgTaO$_3$ [$(1-x)$KNN–xAT] lead-free ceramics with good piezoelectric properties were successfully developed. The effects of the AT on the phase transition behavior and electrical properties of the ceramics were mainly investigated. It was found that all ceramics possess orthorhombic structure at room temperature, and the optimum AT concentration and the denser microstructure results in the improvement of the piezoelectric properties of the ceramics. The $(1-x)$KNN–xAT ($x = 0.08$) ceramic possesses optimum electrical properties ($d_{33} = 183$ pC/N, $k_p = 41\%$, $T_c = 356\,^\circ$C, $T_{o-t} = 158\,^\circ$C, $\varepsilon_r \sim 683$, and $\tan\delta \sim 3.3\%$), and the phase transition behavior of the $(1-x)$KNN–xAT ($x = 0.08$) ceramics is also clearly exhibited by high temperature XRD. These results show that the $(1-x)$KNN–xAT ceramics are promising lead-free piezoelectric materials for piezoelectric applications.

Acknowledgement

The author thanks the support of College of Materials Science and Metallurgy Engineering of Guizhou University.

References

[1] L. Egerton, D.M. Dillon, J. Am. Ceram. Soc. 42 (1959) 438.
[2] R.E. Jaeger, L. Egerton, J. Am. Ceram. Soc. 45 (1962) 209.
[3] Y. Saito, H. Takao, T. Tani, T. Nonoyama, K. Takatori, T. Homma, T. Nagaya, M. Nakamura, Nature 432 (2004) 84.
[4] Y. Guo, K. Kakimoto, H. Ohsato, Appl. Phys. Lett. 85 (2004) 4121.
[5] J.G. Wu, D.Q. Xiao, Y.Y. Wang, J.G. Zhu, L. Wu, Y.H. Jiang, Appl. Phys. Lett. 91 (2007) 252907.
[6] J.G. Wu, Y.Y. Wang, D.Q. Xiao, J.G. Zhu, Z.H. Pu, Appl. Phys. Lett. 91 (2007) 132914.
[7] M. Matsubara, T. Yamaguchi, W. Sakamoto, K. Kikuta, T. Yogo, S. Hirano, J. Am. Ceram. Soc. 88 (2005) 1190.
[8] S.J. Zhang, R. Xia, T.R. Shrout, G.Z. Zang, J.F. Wang, Solid State Commun. 141 (2007) 675.
[9] Y.Y. Wang, Q.B. Liu, J.G. Wu, D.Q. Xiao, J.G. Zhu, J. Am. Ceram. Soc. 92 (2009) 755.
[10] Y.Y. Wang, J.G. Wu, D.Q. Xiao, J.M. Zhu, Y. Jin, J.G. Zhu, P. Yu, L. Wu, X. Li, J. Appl. Phys. 102 (2007) 054101.
[11] Y.F. Chang, Z.P. Yang, Y.T. Hou, Z.H. Liu, Z.L. Wang, Appl. Phys. Lett. 90 (2007) 232905.
[12] J.G. Wu, Y.Y. Wang, D.Q. Xiao, J.G. Zhu, Phys. Stat. Solidi-Rapid Res. Lett. 1 (2007) 214.
[13] B.Q. Ming, J.F. Wang, P. Qi, G.Z. Zang, J. Appl. Phys. 101 (2007) 054103.
[14] J. Yoo, K. Lee, K. Chung, S. Lee, K. Kim, J. Hong, S. Ryu, C. Lhee, Jpn. J. Appl. Phys. 45 (2004) 7444.
[15] J.G. Wu, D.Q. Xiao, Y.Y. Wang, J.G. Zhu, P. Yu, J. Appl. Phys. 103 (2008) 024102.
[16] J. Fu, R.Z. Zuo, X.H. Wang, L.T. Li, J. Phys. D: Appl. Phys. 42 (2009) 012006.
[17] M. Kosec, V. Bobnar, M. Hrovat, J. Bernard, B. Malic, J. Holc, J. Mater. Res. 19 (2004) 1849.
[18] H.L. Du, W.C. Zhou, F. Luo, D.J. Liu, S.B. Qu, Z.B. Pei, Appl. Phys. Lett. 91 (2007) 212907.
[19] J.G. Wu, D.Q. Xiao, Y.Y. Wang, W.J. Wu, B. Zhang, J.G. Zhu, J. Appl. Phys. 104 (2008) 024102.
[20] K. Wang, J.F. Li, N. Liu, Appl. Phys. Lett. 93 (2008) 092904.